Vol. 91 (1997) *ACTA PHYSICA POLONICA A* No. 4

Proceedings of the 3rd ISSSRNS Jaszowiec '96

INVESTIGATION OF ELECTRONIC DENSITY IN C_{60} BY COMPTON SCATTERING

CH. BELLIN, M. MARANGOLO, J. MOSCOVICI[a], G. LOUPIAS[b]

LMCP, Université Paris VI, case 115, 4 place Jussieu, 75252 Paris Cedex 05 and
[a]LPMD, Université Paris XII, 61 av. Gl de Gaulle, 94010 Créteil Cedex and
[b]LURE, bât. 209, Université Paris-Sud, 91405 Orsay Cedex, France

S. RABII

Dpt. Electrical Engineering, Univ. of Pennsylvania, Philadelphia, PA 19104-6390, USA

AND S. ERWIN

Complex Systems Theory Branch, Naval Research Lab., Washington, DC 20375, USA

High-resolution measurements of Compton profiles on C_{60} as well as K_xC_{60} have been carried out using 16 keV photons at LURE (Orsay, France) and at ESRF (Grenoble, France). Theoretical profiles are obtained using the plane wave expansion of wave functions from an *ab-initio* self-consistent field calculation of the energy band-structure. The linear combination of atomic orbitals method within the local-density-approximation has been employed for the calculation. In all cases, the agreement between theory and experiment is excellent. The C_{60} profiles indicate substantially greater delocalization of the ground-state charge density, compared to graphite. We have demonstrated, both by experiment and calculation, that the delocalization in C_{60} is mainly a molecular effect.

PACS numbers: 61.46.+w, 71.90.+q, 78.70.Ck

1. Introduction

C_{60} is one of the members of a novel phase of carbon called the fullerenes, which contain closed-caged structures with different numbers of carbon atoms. In the case of C_{60}, the cage is in the form of a truncated icosahedron, i.e., football shaped and can be crystallized in several different phases [1]. C_{60} molecule is the most symmetric and stable of the many allotropes of carbon and has been subject of intense experimental and theoretical studies in the recent years [2–3]. This molecule crystallises in a face-centered-cubic (FCC) structure, where the C_{60} molecules, located at the lattice sites, are orientationally disordered. Below 260 K, the material makes a transition to a simple cubic, ordered phase. Furthermore, C_{60}

has been intercalated with heavy alkali, K, Rb and Cs, and shown to undergo superconducting transition at relatively high temperatures [4]. In the case of K_xC_{60}, x takes on values of 3, 4 and 6, resulting in a range of conductivity from metallic to insulating, with increasing electron transfer from the alkali atom to the C_{60} cage [5]. It is also possible to co-intercalate C_{60} with two heavy alkali atoms resulting in ordered ternary compounds. In 1991, the appearance of superconductivity at 18 K was reported in K_3C_{60} [4]. The highest superconducting transition temperature obtained so far is 33 K which occurs in $CsRb_2C_{60}$ [6]. There is a number of questions dealing with these compounds such as the nature of charge transfer from the alkali atoms to the carbon cages, the importance of electron–electron correlation and its role in their superconducting behavior. A clear understanding of their electronic structure will answer many of the fundamental questions posed by these novel and interesting materials. We will use the theoretical and experimental study of Compton scattering to provide an understanding of their electronic structure.

A choice of the Compton scattering for synthetic materials investigation is made for very important reasons. First, it is a bulk measurement and at the same time not very sensitive to defects in the solids. The latter is quite important given the nature of the host material. Second, if one subtracts the profile of the host of the intercalated material, many of the systematic errors in the measurement will cancel out leading to an accurate picture of the effects of charge transfer and distortion of initial electronic density of the host. This cancellation of errors also applies to the calculated "difference Compton profiles".

2. Compton scattering

This phenomenon involves the inelastic scattering of incident photons by the electrons. Conservation of energy and momentum, along with the condition that the change in the wavelength of the photon is much smaller than its initial wavelength λ_1 allows us to obtain $\Delta\lambda$, the change in photon wavelength during the scattering process

$$\Delta\lambda = \frac{2h}{mc}\sin^2\left(\frac{\phi}{2}\right) + \frac{2\lambda_1}{mc}\sin\left(\frac{\phi}{2}\right)q,$$

q is the projection of the initial momentum of the electron along the scattering vector e.

The first term which is referred to as the Compton shift is independent of the initial momentum of the electron and is of no interest to us. The second term furnishes us with the momentum density of the electrons in the solid. Within the impulse approximation, the directional Compton profile is defined as follows [7–9]:

$$J(q, e) = \int n(p)d(p \cdot e - q)\mathrm{d}p = \int c(p)c^*(p)d(p \cdot e - q)\mathrm{d}p,$$

where e is the unit vector along the scattering vector, $n(p)$ is the electron momentum density and $\chi(p)$ is the wave function of the electron in momentum space, i.e., the Fourier transform of the wave function in a real space. If the wave functions are represented by their plane wave expansion

$$\Psi_{n,k(r)} = \sum_G C_{n,k}(G)\exp[\mathrm{i}(k + G) \cdot r],$$

where $\boldsymbol{G}$'s are reciprocal lattice vectors, the directional profile can be written as [10]

$$J(q, e) = \frac{1}{N} \sum_{n} \sum_{\boldsymbol{k}} \sum_{\boldsymbol{G}} |C_{n,\boldsymbol{k}}(\boldsymbol{G})|^2 \delta[(\boldsymbol{k} + \boldsymbol{G}) \cdot e - q] \theta(E_n - E_f).$$

The summation $\boldsymbol{G}$ is over all the reciprocal lattice vectors where the $C_{n,\boldsymbol{k}}(\boldsymbol{G})$ is non-negligible. The number of $\boldsymbol{G}$'s required to achieve convergence is related to the size of the primitive unit cell and also increases with the hardness of pseudopotentials. In our experience, it has ranged with 64000 vectors for C_{60}. The summation $\boldsymbol{k}$ is over the symmetry-reduced sector of the Brillouin zone (BZ) and is carried out by calculating the self-consistent wave functions over a grid of $\boldsymbol{k}$'s in the BZ. The summation n is over the occupied states. The function θ cuts off this summation at the Fermi energy in the case where the material is a metal or a semimetal.

3. Experiments

Compton profiles have been measured for both C_{60} powder and single crystal samples, above and below phase transition temperature. The powdered sample was provided by A. Rassat and C. Fabre (Lab. Chimie-ENS Ulm, Paris) and the single crystal by J. Godard and H. Szwarc (Univ. Orsay, France).

A three axes focusing high resolution spectrometer [11] has been installed on the wiggler beam line at "Laboratoire pour l'Utilisation du Rayonnement Électromagnétique" (LURE), using synchrotron radiation beam monochromatised to select photons of 16 keV energy by Bragg reflection from a double crystal 220 silicon monochromator. The photons are back-scattered by the sample of C_{60} powder, 4 mm thick, energy analysed by means of a Si (440) Cauchois curved analysing crystal and focused to a single point on the Rowland circle. They are detected by a position sensitive detector which is situated tangentially to the focal circle. For this reason, the detector is used to record the entire Compton spectrum at the same time. 3 millions of events have been accumulated in the Compton peak between $q = -2$ to 2 atomic units of momentum (a.u.). The separation between data points is equivalent to 0.03 a.u when expressed in terms of the electron momentum scale. The resolution function is measured from the full width at half maximum of the thermal diffuse scattering (TDS) peak, which is 0.16 a.u. The TDS peak can be fitted by a Gaussian curve whose standard deviation, σ, is equal to 0.07 a.u. of momentum.

For comparison, directional Compton profiles, whose scattering vectors $\boldsymbol{K}$, are perpendicular and parallel to c axis, have been measured on a highly oriented pyrolitic graphite (HOPG). HOPG is composed of domains whose c axes are parallel within half a degree, but are randomly oriented with respect to each other in the basal plane. Thus two measurements provide the directional profile (DP) along the c axis and an average profile in the basal plane.

Measurements on C_{60} single crystal were carried out with a similar spectrometer installed on the main arm of the κ diffractometer, at the ESRF on the beam line 2 (ID 11) [12]. The optics of beam line 2 are designed in order to obtain a small spot of 0.2×0.2 mm^2 size on the sample, which is an ideal situation for studying small crystals such as C_{60} ones. A resolution function is the same as the one described above. Profiles for 8 different directions of the scattering vector $\boldsymbol{K}$, with

respect to crystallographic directions, were measured at 2 temperatures, below and above the structural transition, i.e. room and liquid nitrogen temperatures.

At energies such as 16 keV, used for light compounds, the system is very sensitive to parasitic photons scattered by air and any material in the beam paths. Such photons are also energy analysed by the crystal analyser and give a contribution to the Compton profile of interest [13]. A special housing for the sample and analyser has been designed in order to refine experimental conditions, as shown in Fig. 1.

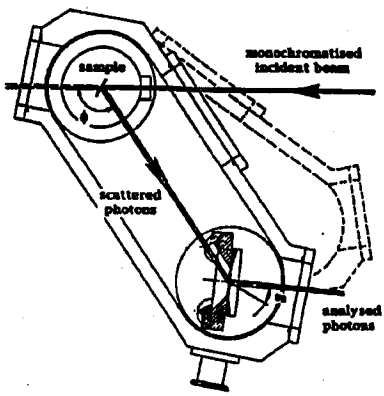

Fig. 1. Sample and analyser housing.

For all the Compton profiles, the multiple scattering contributions were calculated using a Monte Carlo simulation and taking account of the beam polarization [14]. In the present conditions, the contribution of double processes to the measured profile was 2% and the triple scattering was negligibly small. The final experimental profile is obtained by subtracting the simulated double scattering profile from the measured results.

4. Results and discussion

The contribution of the core electrons to the total Compton profile is quite extended in momentum space in comparison to that of the valence electrons. This allows for the separation of these two contributions to the experimentally measured Compton profiles and to look at details of the valence charge density, i.e., of electrons responsible for the properties of interest in solid state physics. The core Compton profile is evaluated beyond the impulse approximation using the quasi-self-consistent method (QSCF) [15] which takes into account the potential seen by the recoil electrons. Since the theoretical results are obtained using the pseudopotential formalism, there is no contribution to the theoretical profiles from the core electrons, making the comparison quite easy.

4.1. Powdered C_{60} sample

In the case of powdered C_{60} sample, the theoretical profile was obtained by averaging the calculated DP for 001, 111, 011, 112 directions. For graphite,

the measurements were performed using a HOPG sample. As a consequence, the Compton measurements provide DP along the c axis but a powder profile in the basal plane. In order to compare these experimental results with our calculations, the theoretical in-plane profile was obtained by averaging the DP calculated for eight directions, spanning the irreducible sector at intervals of 4.28°. Then, the theoretical profiles were convolved with the experimental resolution function.

All the valence profiles (VP) are normalised to 4, the number of electrons per carbon atom. Theoretical and experimental results for the difference between the average C_{60} profile and the graphite profile, measured with scattering vector parallel to c axis, are compared in Fig. 2, eliminating the effect of the systematic isotropic errors in both theory and experiment. It is seen that agreement between the calculated and measured differences is excellent.

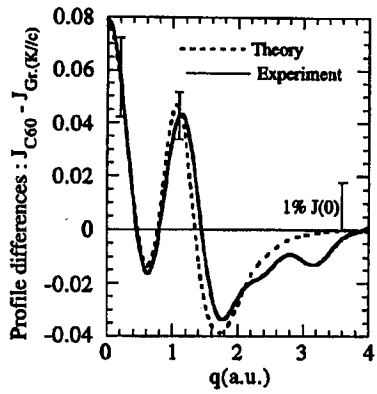

Fig. 2. Comparison of Compton profile differences $\Delta J(q)$. The error bar is due to the statistical accuracy.

The observed narrowness of C_{60} profile with respect to both directional Compton profile of graphite, can be interpreted as a larger delocalization of valence electrons in the solid C_{60} than in graphite. In order to estimate the percentage of the delocalised electrons, we calculate the areas under the Compton profiles for small values of momentum, typically $q < p_F$, the Fermi momentum of graphite (1.4 a.u.). The difference between these areas for C_{60} and graphite indicates that approximately 2% of the electrons are involved [16]. In order to answer the question of origin of the observed delocalization in the C_{60} solid and evaluating the solid state effect in this molecular solid, we have compared the electron density in the actual solid and that obtained for a fictitious solid with an expanded lattice, corresponding to decoupled molecules. The wave functions were calculated for a lattice constant equal to 1.2 times the equilibrium value. In this fictitious solid, a distance between closest carbon atoms of two different balls increases to 4.93 Å, i.e., 1.6 times the distance (3.08 Å) in the actual solid. At this lattice constant, the C_{60} complexes are essentially decoupled and the wave functions correspond to molecular C_{60}. Due to the small magnitude of the reciprocal lattice vectors, for the expanded lattice, it was necessary to retain 64 000 plane waves in the Fourier

expansion of the wave functions, in order to achieve convergence. The resulting Compton profile, calculated from these wave functions is taken to be the molecular C_{60} profile. Only a slight difference is observed: the value of the average profile at $q = 0$ changes by only 0.17% between the solid and the molecular case, indicating that the additional delocalization in C_{60}, over graphite, as seen in Compton scattering, is mainly concentrated on C_{60} balls.

This assumption is supported by the low temperature measurement (liquid nitrogen). At that temperature, the molecules are no more orientationally disordered and which leads us to expect stronger inter-ball bonds in this ordered phase, resulting in a substantial change in the Compton profile. The difference between the two C_{60} measurements at room and low temperatures is no larger than the statistical error bar for any value of q, indicating the weakness of inter-ball bonds.

4.2. C_{60} single crystal

In the case of the C_{60} single crystal, a direct comparison between theoretical and experimental DPs is possible. In particular, the electronic density anisotropy can be exhibited by difference of DPs. Figure 3 shows the tight anisotropies obtained by both theory and experiment.

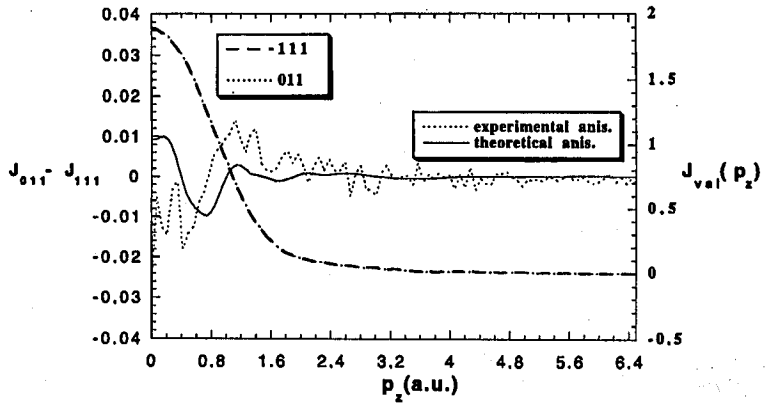

Fig. 3. Directional Compton profiles of C_{60} and both related experimental and theoretical anisotropies.

Even if the details of the experimental features are not well described by theory, we can notice that the orders of magnitude are similar, supporting the fact that solid effect is surprisingly weak in C_{60}.

In conclusion, the present C_{60} results are very important for the intercalated compounds understanding. In particular, the potassium compound (K_3C_{60}, K_4C_{60}, K_6C_{60}) samples, provided by C. Hérold, Ph. Lagrange and J.F. Marêché (Univ. of Nancy I), were recently measured at LURE. The differences between profiles of K_xC_{60} and C_{60} have been done for both experiment and local-density-approximation theory and they show a good agreement. These potassium depending

differences are dominated by bands resulting from $3p$ potassium levels hybridized with C_{60} valence electrons, leading to a large distortion electronic density of C_{60}.

References

[1] W. Krätschmer, *Synth. Met.* **70**, 1309 (1995).

[2] H.W. Kroto, A.W. Allaf, S.P. Balm, *Chem. Rev.* **91**, 1213 (1991); K. Prassides, H. Kroto, *Phys. World* **44**, (1992).

[3] C.T. Chen, L.H. Tjeng, P. Rudolf, G. Meigs, J.E. Rowe, J. Chen, J.P. McCauley Jr, A.B. Smith III, A.R. McGhie, W.J. Romanow, E.W. Plummer, *Nature* **352**, 603 (1991); L.D. Lamb, D.R. Huffman, *J. Phys. Chem. Solids* **54**, 1635 (1993); J.E. Fischer, P.A. Heiney, *J. Phys. Chem. Solids* **54**, 1725 (1993).

[4] A.F. Hebard, M.J. Rosseinsky, R.C. Haddon, D.W. Murphy, S.H. Glarum, T.T.M. Palstra, A.P. Ramirez, A.R. Kortan, *Nature* **350**, 600 (1991).

[5] S.C. Erwin, in: *Buckminsterfullerenes*, Eds. W.E. Billups, M.A. Ciufolini, VCH Publishers, New York 1993, p. 217.

[6] K. Tanigaki, I. Hirosawa, T.W. Ebbesen, J. Mizuki, Y. Shimakawa, Y. Kubo, J.S. Tsai, S. Kuroshima, *Nature* **356**, 419 (1992).

[7] M.J. Cooper, *Rep. Prog. Phys.* **48**, 415 (1985).

[8] P. Eisenberger, P.M. Platzman, *Phys. Rev. A* **2**, 415 (1970).

[9] S. Rabii, J. Chomilier, G. Loupias, *Phys. Rev. B* **40**, 10105 (1989).

[10] P. Rennert, *Phys. Status Solidi B* **105**, 567 (1981).

[11] G. Loupias, J. Petiau, A. Issolah, M. Schneider, *Phys. Status Solidi B* **102**, 79 (1980).

[12] Å. Kvick, *ESRF Beamline Handbook*, ESRF, 1994 p. 61.

[13] Ch. Bellin, J. Frouin, G. Loupias, *J. Synchrotron Rad.* **2**, 315 (1995).

[14] J. Chomilier, G. Loupias, J. Felsteiner, *Nucl. Instrum. Methods A* **235**, 603 (1985).

[15] A. Issolah, B. Lévy, A. Beswick, G. Loupias, *Phys Rev. A* **38**, 4509 (1988); A. Issolah, Y. Garreau, B. Lévy, G. Loupias, *Phys Rev. B* **44**, 11029 (1991).

[16] J. Moscovici, G. Loupias, S. Rabii, S. Erwin, A. Rassat, C. Fabre, *Europhys. Lett.* **31**, 87 (1995).